Translational Oncology 24 (2022) 101487

Contents lists available at ScienceDirect

Translational Oncology

journal homepage: www.elsevier.com/locate/tranon

LncRNA C9orf139 can regulate the progression of esophageal squamous carcinoma by mediating the miR-661/HDAC11 axis

Xiaojie Yang [a,b,1], Zhimin Shen [a,b,1], Mengyue Tian [c], Yukang Lin [a,b], Liming Li [a,b], Tianci Chai [b,d], Peipei Zhang [a,b], Mingqiang Kang [a,b,*], Jiangbo Lin [a,b,*]

[a] Department of Thoracic Surgery, Fujian Medical University Union Hospital, No. 29 Xinquan Road, Fuzhou 350001, China
[b] Key Laboratory of Cardio-Thoracic Surgery (Fujian Medical University), Fujian Province University, Fuzhou, Fujian, China
[c] Key Laboratory of Ministry of Education for Gastrointestinal Cancer, The School of Basic Medical Sciences, Fujian Medical University, Fuzhou, China
[d] Department of Cardiovascular Surgery, Fujian Medical University Union Hospital, Fuzhou, China

ARTICLE INFO

Keywords:
C9orf139
Esophageal squamous carcinoma
miR-661
HDAC11
Progression

ABSTRACT

Increasing evidence has indicated that long non-coding RNAs (LncRNAs) play multiple functions in the development of cancer and function as indicators of diagnosis and prognosis. This aim of this study was to investigate the roles LncRNA C9orF139 had in the progression of esophageal squamous carcinoma (ESCC). We found C9orf139 was highly expressed in ESCC and knock down the expression of C9orf139 significantly suppressed cell proliferation, promoted apoptosis, and inhibited migration and invasion. C9orf139 was able to negatively regulate miR-661 expression. At the same time, HDAC11 expression was negatively regulated by miR-661. The C9orf139/miR-661/HDAC11 axis was further involved in regulating the expression of the NF-κB signaling pathway. The association between the C9orf139 knockdown and the reduced tumor growth and size was observed during *in vivo* study. C9orf139 is highly expressed in ESCC, and is thus qualified to be used as a potential diagnostic and prognostic marker for ESCC. Its promotion of ESCC progression is achieved by mediating the miR-661/HDAC11 axis.

Introduction

Esophageal cancer (ESCA) is one of the most common cancers in the world, accounting for 11% of total cancer diagnoses each year [1,2]. According to histopathological classification, esophageal carcinoma is mainly divided into esophageal squamous carcinoma (ESCC) and esophageal adenocarcinoma (EA). ESCC accounts for more than 90% of the confirmed cases of esophageal cancers in China [3,4]. Although there are currently several treatments for ESCC that have been applied clinically [5,6], there are still many limitations which have been brought about by technological development and lack of a more detailed understanding of the pathogenesis of ESCC, so the 5-year survival rate of it is only 22–30% [7]. The early diagnosis and intervention of diseases are of great significance in the treatment of diseases. Therefore, it is important to explore the molecular mechanism of ESCC occurrence and development and, for the treatment of ESCC, to search for molecular targets by controlling the malignant development of ESCC to improve of prognosis and survival rate.

In the human genome, only 2% of expressed transcripts are protein-coding RNAs, while the rest are non-coding RNAs, of which long non-coding RNAs (LncRNAs) account for the largest proportion, about 80% [8,9]. More and more studies have shown that changes in the LncRNA expression profile are highly correlated with the progression of various cancers [10–12]. What is more interesting is that the interaction between LncRNAs and microRNAs (miRNAs) has been mentioned in these studies. For example, LncRNA H19 is able to interact with miR-138 and miR-200a to promote epithelial-mesenchymal transformation (EMT) in colorectal cancer [13]; LncRNA PAGBC is able to inhibit the functions of miR-133b and miR-511 and promote the occurrence of gallbladder tumors [14]. In general, LncRNAs combined miRNA and act as miRNA sponges which would reduce miRNA regulatory capacity [15]. As an important member of the LncRNA family, C9orf139 was found to be differentially expressed in various tumors, and is expected to become a potential target for pancreatic cancer therapy [16]. Also, C9orf139 was highly expressed in pancreatic cancer and promoted pancreatic cancer cell growth by mediating the miR-663a /Sox12 axis [17]. In addition,

* Corresponding authors at: Department of Thoracic Surgery, Fujian Medical University Union Hospital, No. 29 Xinquan Road, Fuzhou 350001, China.
E-mail addresses: mingqiang_kang@126.com (M. Kang), jiangbolin99@163.com (J. Lin).
[1] These authors contributed equally to this work.

https://doi.org/10.1016/j.tranon.2022.101487
Received 11 May 2022; Received in revised form 4 July 2022; Accepted 9 July 2022

bioinformatics analysis of patients with pancreatic ductal adenocarcinoma (PDCA) indicated that C9orf139 was a promising prognostic indicator for PDCA [18].

MiRNAs, as endogenous non-coding small RNAs, can inhibit gene expression by inhibiting mRNA translation and participate in post-transcriptional regulation of genes [19]. In recent years, the role of miRNAs in tumorigenesis and development has been extensively reported. Differences in the expression of miR-661 have been detected in different tumors and physiological functions which have been shown in diverse cells [20,21]. TUSC2P suppresses the tumor function of esophageal squamous cell carcinoma by regulating TUSC2 by miR-661 from binding to TUSC2 [22]. However, the role of miR-661 in ESCC has not been reported in detail.

HDAC11, the newest member of the 11 human zinc-dependent HDACs, is also the smallest protein in this family and has the least characterized biological function. HDAC11 has been implicated in diverse immune functions [23], myoblast differentiation [24], metabolism, and obesity [25]. Its depletion has been reported to promote cell death and inhibit metabolic activity in HCT-116 colon, MCF7 breast, PC-3 prostate, and SK-OV-3 ovarian cancer cell lines [26]. In our study, we aimed to make clear the molecular role of C9orfl39 in the tumorigenesis of ESCC and identify its potential interaction with miR-661/HDAC11 axis.

Materials and methods

Cell lines, culture and transfection

Human esophageal cancer cell line TE-1, human esophageal cancer cell line ECA109, and human embryonic kidney cell 293T were purchased from Beyotime, China. TE-1 cells were cultured in RPMI 1640 with 10% FBS (Gibco, Australia) and 1% penicillin/streptomycin (Invitrogen, USA). ECA109 and 293T were cultured in DMEM with 10% FBS (Gibco, Australia) and 1% penicillin/streptomycin (Invitrogen, USA). All cells were cultured in an incubator suitable for 37°C, 5% CO2, and 95% humidity. shRNA-C9orf139, miR-661 mimic, and anti-miR-661 inhibitor were synthesized by the company (50OD, purified by HPLC) and self-diluted for use. The pcDNA3.1-HDAC11 was derived from a subclone of the chemically synthesized CDS region of pcDNA3.1. Cells were collected, counted, and seeded into 6-well plates the day before transfection. Cell transfection was performed by using lipofectamine 2000 (Invitrogen, Carlsbad, CA, USA), in accordance with the manufacturer's protocol. DMEM with 10% FBS was added to each well at 6 h following transfection. All shRNA, miRNA and anti-miRNA inhibitors were purchased from Genecopoeia (USA).

RNA extraction and RT-qPCR

Total RNA was extracted by using kit reagents to separate nuclear and cytoplasmic RNA without cross-contamination (RNA subcelluar isolation kit, Active Motif, USA). The total RNA was collected using kit reagents and the mass of total RNA was evaluated by Nanodrop 2000 spectrophotometer (Thermofisher Scientific, USA). Reverse transcription of 1.0 μg total RNA to cDNA and qPCR was performed by using the SYBR Green MasterMinds Kit Testing on the testing system platform (Biosystems 7500, ABI, USA). The gene expression data was performed by $2-\Delta\Delta Ct$ method to analyze the relative quantity. All primers are commercially available from Thermofisher Scientific (USA).

Cell Counting Kit-8 (CCK-8) assay

Cells were inoculated 4000 cells/well into 96-well plates (100 ul volume); 24 h after cell inoculation, medium was removed and 100ul of fresh RPMI1640 medium (containing 2%FBS) was added. Lipofilter was about 0.6 ul. 24.4 ul was mixed with RPMI1640 medium (excluding FBS), and incubated at room temperature for 5 min. The prepared siRNA was about 50pmol (2ul) (or 0.25ug PCDNA3.1 plasmid containing the GENE CDS region) and mixed with 23ul RPMI1640 medium (excluding FBS). The 2 prepared tubes of solution were gently mixed and incubated at room temperature for 20 min, and then added into the wells; After 6 h of incubation, medium was removed and 150ul of fresh RPMI1640 medium (containing 10%FBS) was added for further culture. After 72 h of incubation, 10ul CCK8 reagent was added for further incubation for 1–4 h. The absorbance was measured at 450nm.

Clone formation

A 6-well plate was taken, and the target cells of the exponential growth period were inoculated: 1000 cells/well. The NC control group (or Ctrl group) and experimental group were set, and the number of cells was able to be adjusted appropriately according to experimental needs. 24 h after cell inoculation, fresh RPMI1640 medium 1500ul (containing 2%FBS) was replaced. The lipofilter was about 5.0ul, mixed with 250ul RPMI1640 medium (containing 2%FBS), and incubated at room temperature for 5min. The prepared siRNA was about 50pmol(2ul) or 0.25ug plasmid, and was mixed with 250ul RMI1640 medium (containing 2%FBS). The 2 prepared tubes of solution were gently mixed, then left to incubate at room temperature for 20 min before being added to cells. After 6h of culturing, medium was removed and 2000ul of fresh RMI1640 medium (containing 10%FBS) was added. After 7–10 days of continuous incubation, the number of clones was observed under a microscope, photographed, and counted.

Transwell assay

A 24-well Transwell plate was taken (pretreated with 0.2ml matrix glue for 1h), and the target cells (containing 5%FBS) in the exponential growth period were inoculated in the upper chamber: 10000 cells /250ul/well, then the NC control group and experimental group were set. Each group was repeated in with three multiple wells. 4h after cell inoculation, 2.4ul lipofilter was taken, 47.6ul was mixed in RPMI1640 medium (containing 5%FBS), and incubated at room temperature for 5 min. The prepared siRNA or miRNAs were about 50pmol(2ul) or 0.25ug pcDNA3.1-HDAC11 plasmid, and was mixed with 46ul RPMI1640 culture base (containing 5%FBS). The 2 prepared tubes of solution were mixed and incubated at room temperature for 20min, added into the cells and mixed gently again. After 6–12 h of culturing, 300ul of fresh RPMI1640 medium (containing 5%FBS) was replaced, and 500ul RPMI1640 medium (containing 20%FBS) was added into the lower chamber to continue culturing. After 48 h of culturing, the upper chamber was removed and the cells attached to the upper surface of the upper chamber were gently scraped with cotton swabs. The cells on the lower surface were treated and stained with crystal violet staining, and these cells were observed under a microscope then photographed.

Annexin V-FITC assay

Cells were inoculated during the exponential growth period: 10,0000 cells/well, the NC control group and experimental group were set. Each group was repeated in with three multiple wells. 24 h after cell inoculation, medium was removed and 500ul of fresh RPMI1640 medium (containing 2%FBS) was added 2.4ul lipofilter was taken, 47.6ul was mixed with RPMI1640 medium (containing 2%FBS), and stood at room temperature for 5 min. The prepared siRNA was about 50pmol(2ul) or 0.25ug plasmid, and mixed with 46ul RPMI1640 medium (containing 2%FBS). 2 tubes of solution were gently mixed, then held at room temperature for 20 min, then add into cells. After 6h culture, 500ul of fresh RPMI1640 medium (containing 10%FBS) was replaced. After 72 h of culturing, cells were centrifuged at 300g for 5 min. The cells were resuspended by pre-cooled PBS and centrifuged at 300g for 5 min. PBS was discarded and 100ul 1*Binding buffer was added to resuspend cells. Annexin V-FITC 5ul was added, mixed gently, held in the dark at room

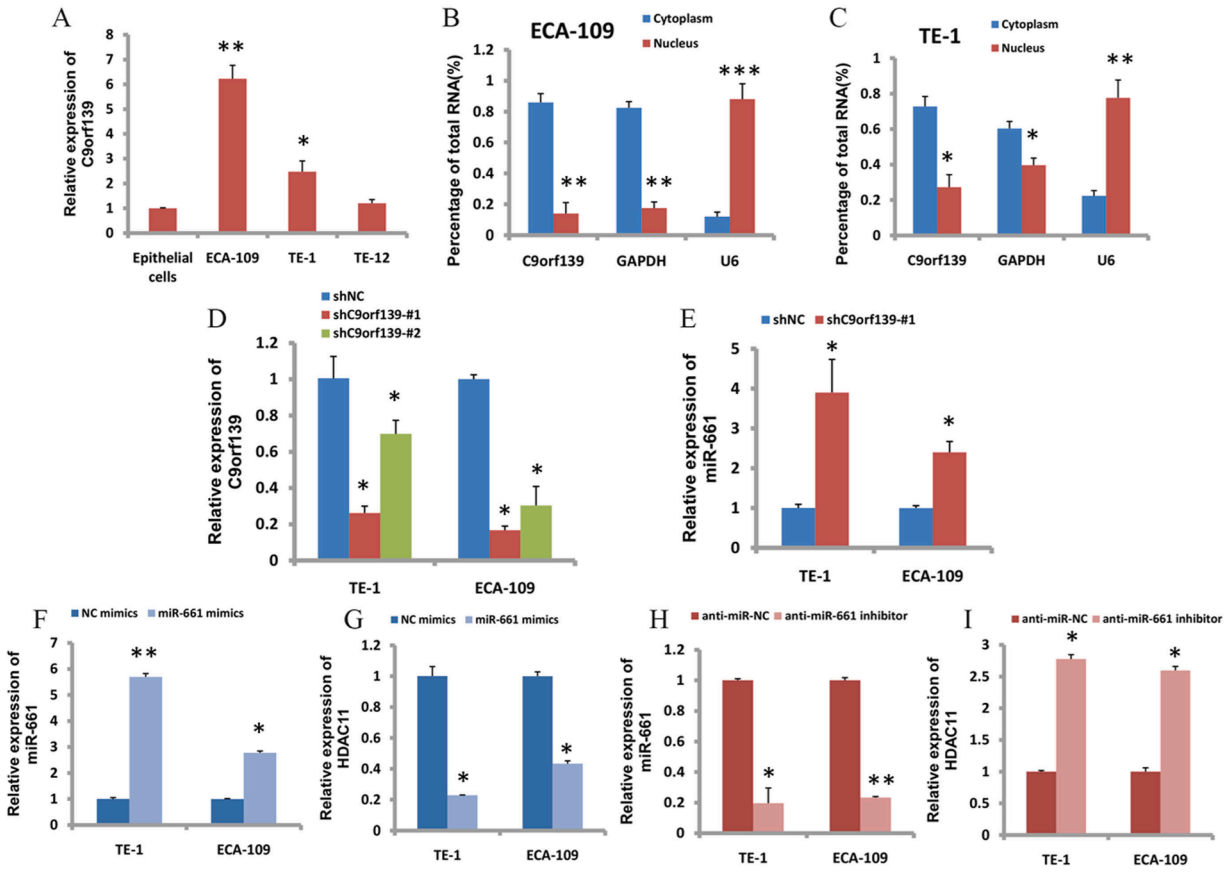

Fig. 1. *Interactions of C9orf139/miR-661/HDAC11.* (A) qPCR assay was used to detect the expression of C9orf139 in normal esophageal cells which called ECA109, TE-1 and TE-12. (B, C) Cell localization of C9orf139 in TE-1 and ECA109 cells. (D) The shC9orf139-#1 and shC9orf139-#2 infection efficiency of TE-1 cells and ECA109 cells were analyzed by qPCR to compare with shNC group. (E) Effect of C9orf139 knockdown on miR-661 in TE-1 and ECA109 cells. (F-G) Effect of miR-661 mimic on HDAC11 gene expression. (H-I) Effect of anti-miR-661 inhibitor on HDAC11 gene expression. All datas were presented as mean ± SD. (*$p < 0.05$, **$p < 0.01$, ***$p < 0.001$ vs. relative controls).

temperature for 10–15 min. 400ul 1*Binding Buffer was added, mixed evenly and placed on ice for flow detection within 1h.

Dual luciferase activity detection

After 48 h of transfection, the cells were washed gently with PBS, then 200ul cell lysis solution was added to each well, and was incubated on ice for 5–10 min to fully lyse the cells. As instructed in the kit instructions (Shanghai YEASEN Biotechnology), luciferase substrate was prepared and kept on ice. 20ul cell lysate and 100ul of firefly luciferase reaction solution was added into each well of the 96-well plate. Finally, the plate was put into the plate tester to detect firefly luciferase activity. After the firefly luciferase activity was detected, 100ul of aquiferase reaction solution was added to each well and aquiferase activity was detected.

Western blotting assay

After the experimental cells were washed twice with PBS solution, 100ul cell lysis buffer (containing 1% protease inhibitor 1%EDTA) was added, fully mixed at room temperature for 30 s and centrifuged at 13,000rpm for 5 min. 20ul of supernatant was taken after centrifuging to thoroughly mix with 5ul of protein loading buffer. The samples were suspended in boiling water for 5 min, and then some samples were taken. After electrophoresis, the membrane was transformed. PVDF membrane was blocked with blocking solution and incubated with IKK antibody(ab32041) (1:500), IkB antibody(ab76429)(1:500), NF-κB antibody(ab32360) (1:1,000), HDAC11 antibody (ab18973)(1:1,000), NCOR1 antibody(ab3482) (1:2,000), and GAPDH antibody (ab8245) (1:3,000), .\ at 37°C for 2 h or 4°C overnight. Then, the membrane was washed and incubated with the goat anti-rabbit IgG HRP antibody (ab6721) (1:3,000) for 1h at 37°C. After washing the membrane, a chemiluminescence imager was used for chemiluminescence.

Mouse xenograft assay

The effects of C9orf139 on tumorigenesis and growth *in vivo* were detected via mouse xenograft assay. We used twenty 5 to 6-week-old female NU-Foxn1nu nude mice (Vital River Laboratory Animal Technology Co., Ltd., Beijing, China) for the mouse xenograft assay. A total of 3×10^6 TE-1-NC cells or C9orf139-knockdown stable TE-1 cells were used to inject into the right or left oxter of female NU-Foxn1nu nude mice, respectively [17]. Tumor size and weight were determined with calipers and balanced twice a week. After 53 days, the mice were executed and the tumors were removed. The formula $V = (W\ 2 \times L)/2$ was used to calculate the tumor volume. V is the tumor volume, W is the tumor width, and L is the tumor length. Tumor size was presented as mean ± standard deviation (SD).

Protein-protein interaction network

The PPI interaction networks between the DEGs were constructed using the Search Tool for the Retrieval of Interacting Genes (STRING) database (http://string-db.org/) [27]. Firstly, the DEGs were typed into the database. Then, high-resolution bitmaps were displayed and downloaded from the webpage. Only these interactors with a combined

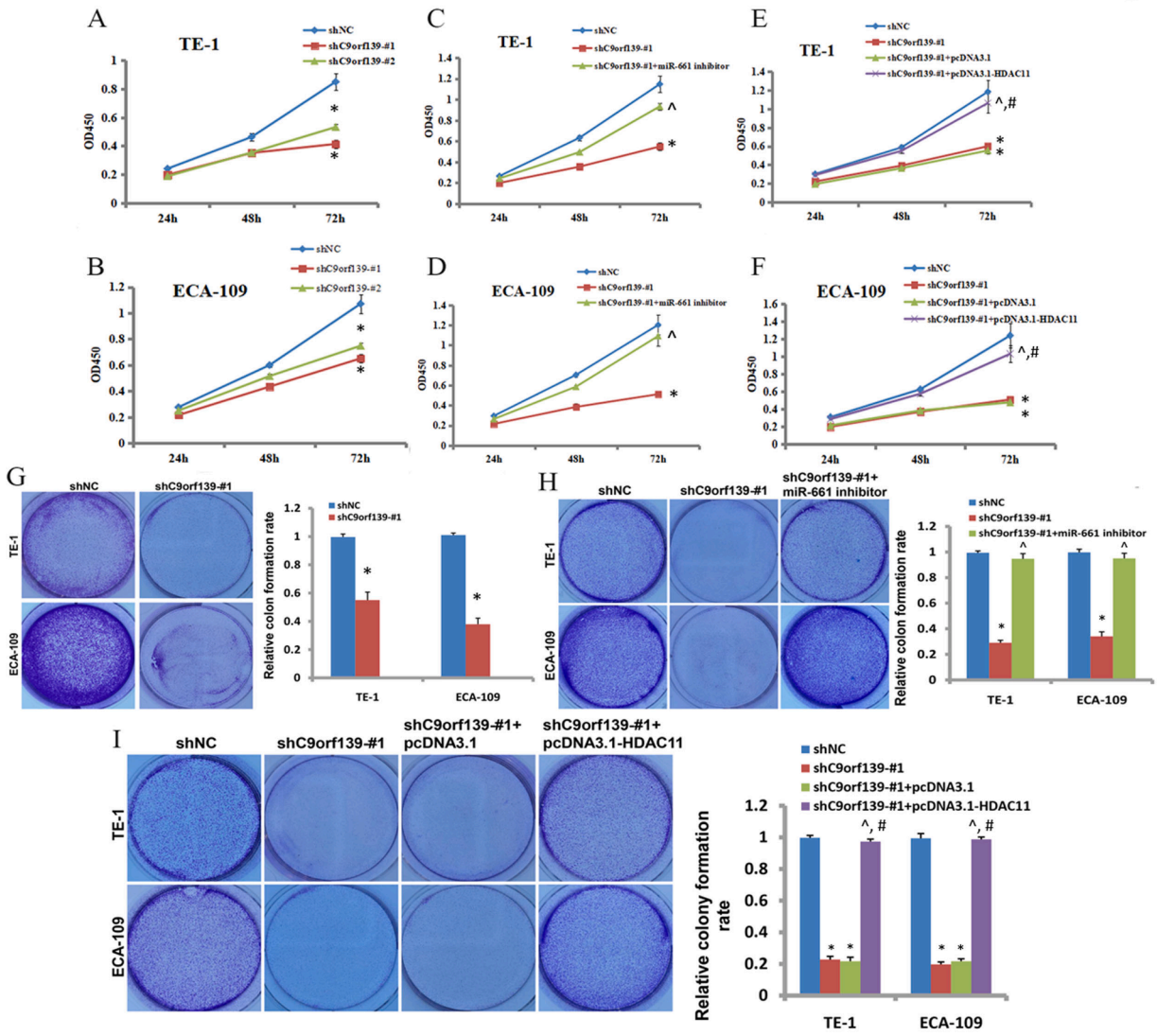

Fig. 2. *C9orf139/miR-661/HDAC11 regulated cell proliferation and clonal formation.* (A) Proliferation of TE-1 cells after transfection with C9orf139 knockdown plasmid. *$p < 0.05$ vs. shNC. (B) Proliferation of ECA109 cells after transfection with C9orf139 knockdown plasmid. *$p < 0.05$ vs. shNC (C-D) Cells proliferation were detected by CCK8, and growth inhibition induced by shC9orf139-#1 was removed after transfection with miR-661 inhibitor. *$p < 0.05$ vs. shNC, ^$p < 0.05$ vs. shC9orfl39#1. (E, F) Cells proliferation were detected by CCK8, and growth inhibition induced by shC9orf139-#1 was relieved after overexpression of HDAC11. *$p < 0.05$ vs. shNC, ^$p < 0.05$ vs. shC9orfl39#1, #$p < 0.05$ vs. shC9orfl39#1+ pcDNA3.1. (G-I) Same as the above experimental groups, clone formation ability was detected and counted. *$p < 0.05$ vs. shNC, ^$p < 0.05$ vs. shC9orfl39#1, #$p < 0.05$ vs. shC9orfl39#1+ pcDNA3.1. All data were presented as mean ± SD.

confidence score ≥ 0.4 were shown in the bitmap.

Statistical analysis

All experiments were repeated at least 3 times during the study period. Statistical analysis was performed using the GraphPad Prism 8 software (GraphPad Software, Inc., La Jolla, CA, USA). All datas are expressed as mean ± SD unless otherwise stated. The main statistical methods were tested with one-way ANOVA ($p < 0.05$ was considered significant in statistic).

Results

Interactions of C9orf139/miR-661/HDAC11

First, we detected the expression of C9orf139 in normal esophageal epithelial cells and esophageal carcinoma cells (ECA109, TE-1 and TE-12). qPCR results showed that the expression of C9orf139 was significantly increased in esophageal cancer cells, especially in the ECA109 cell line (Fig. 1A). In addition, we detected the cytoplasmic distribution of C9orf139 in ECA109 (Fig. 1B) and TE-1 (Fig. 1C) cell lines and found that the distribution of C9orf139 in the cytoplasm of the two cancer cells was much higher than the distribution in the nucleus. Subsequently, we constructed a shRNA-C9orf139 vector and transfected the TE-1 and ECA109 cell lines. The ShC9orf139-#1 fragment with a better knockdown effect (over 70%) was selected for subsequent experiments (Fig. 1D). It was interesting to note that miR-661 was significantly elevated after down-regulation of C9orf139 gene expression (Fig. 1E). Therefore, miR-661 mimic and anti-miR-661 inhibitor molecules were constructed in an attempt to search for downstream molecules of miR-661 inhibitors. After miR-661 expression was increased or decreased, HDAC11 gene expression was decreased or increased, and there was an inverse correlation between the two (Fig. 1F, I).

C9orf139/miR-661/HDAC11 regulated cell proliferation

After determining the intermolecular interaction of C9orf139/miR-661/HDAC11, we first explored the function of this signal axis. As

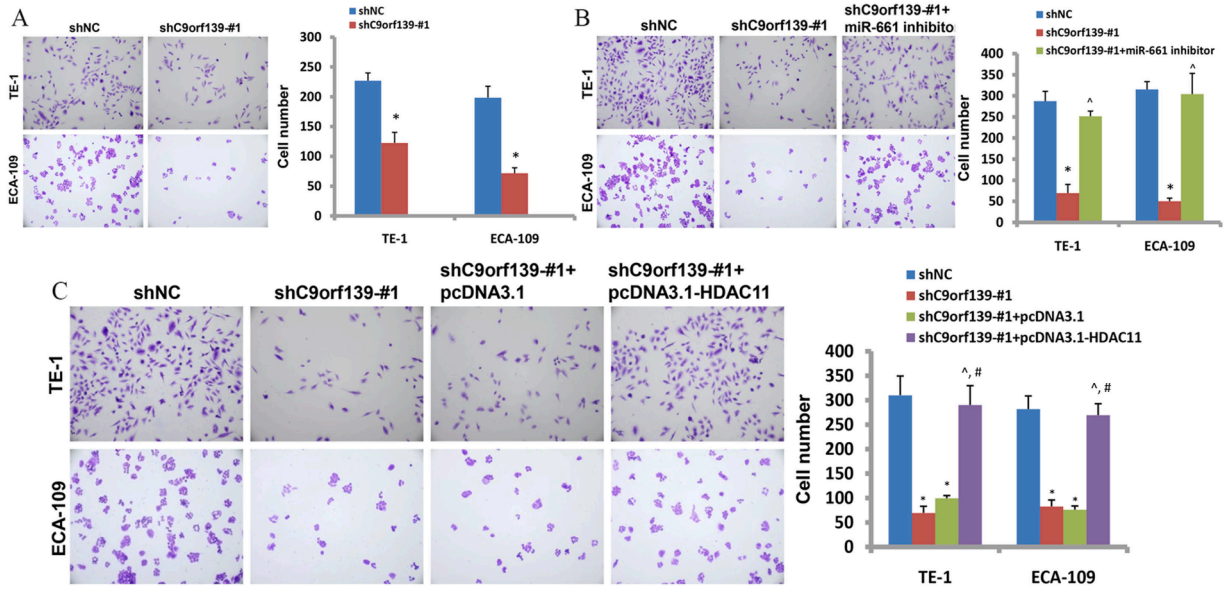

Fig. 3. *C9orf139/miR-661/HDAC11 regulated ESCC cell invasion.* (A) Tumor invasion test: The invasion of tumor cells was weakened by knocking down the expression of C9orf139 gene. $*p < 0.05$ vs. shNC. (B) Tumor invasion test: Compared with shNC, the tumor invasion ability of shC9orf139-#1 group was reduced, and the invasion ability was recovered after co-transfection with Mir-661 inhibitor. $*p < 0.05$ vs. shNC, $\hat{}p < 0.05$ vs. shC9orfl39#1. (C) Tumor invasion assay: Compared with shNC, the tumor invasion ability of shC9orfl39-#1 group decreased, and the invasion ability was restored after co-transfection with pcDNA3.1-HDAC11. $*p < 0.05$ vs. shNC, $\hat{}p < 0.05$ vs. shC9orfl39#1, $\#p < 0.05$ vs. shC9orfl39#1+ pcDNA3.1. All data were presented as mean ± SD.

shown in Fig. 2A, the proliferation ability of TE-1 was significantly reduced after down-regulation of C9orf139 expression, which was consistent in ECA109 cells (Fig. 2B). The proliferation ability of cells was partially restored, and the inhibition caused by the down-regulation of C9orf139 was relieved to a certain extent, after the inhibition of miR-661 expression. (Fig. 2C, D). Overexpression of HDAC11 led to the same results (Fig. 2E, F). Similarly, after the expression of C9orf139 was knocked down, the clonogenesis ability of the cells was decreased (Fig. 2G). Inhibition of miR-661 or overexpression of HDAC11 resulted in the release of inhibition and partial recovery of clonogenesis (Fig. 2H, I).

C9orf139/miR-661/HDAC11 and tumor invasion

In previous experiments, we found that the C9orf139/miR-661/HDAC11 signaling axis regulated the proliferation of esophageal cancer cells. Further, we analyzed the relationship between this signal axis and tumor invasion ability. We pre-inoculated 0.2ml Matrigel (mainly composed of laminin and collagen type Ⅳ) at the bottom of the chamber and inserted the cells according to the number of 1×10^5 cells. After grouping, the cells were cultured for 48h and observed by crystal violet staining. The results showed that the invasion ability of both TE-1 and ECA109 cells was significantly reduced after the expression of C9orf139 was down-regulated (Fig. 3A). Reduced miR-661 expression or the up-regulation of HDAC11 both, to a large extent, restored the invasion ability of tumor cells (Fig. 3B, C).

C9orf139 knockdown induced apoptosis

Similarly, we used the previous grouping model to analyze the effect of C9orf139 on the apoptosis of esophageal cancer cells. Much like in previous results, knockdown C9orf139 remarkably increased the apoptosis rate of TE-1 and ECA109 cells (Fig. 4A, B). When miR-661 was inhibited, the apoptosis rate of tumor cells was dramatically reduced (Fig. 4C, D), and the results were consistent with the one after HDAC11 was upregulated (Fig. 4E, F).

Signal transduction mechanism between C9orf139/miR-661/HDAC11

Our study found that the C9orf139/miR-661/HDAC11 signal axis was closely related to the proliferation, invasion, and apoptosis of esophageal cancer cells. Therefore, the signal transduction mechanism between the signal axis and the molecular pathways that induced cell proliferation, apoptosis and other related changes became the key which urgently needed to be solved. First, we validated the molecular interactions among C9orf139, miR-661 and HDAC11 by using a dual-luciferase system. As shown in Fig. 5A and B, miR-661 mimic significantly reduced luciferase expression driven by C9orf139, while luciferase expression recovered after miR-661 mutation. Similarly, miR-661 mimic significantly lessened luciferase expression driven by HDAC11-3-UTR, and luciferase expression recovered after site mutation (Fig. 5C, D). In addition, miR-661 mimic inhibited HDAC11-3-UTR-driven Luciferase expression in TE-1 cells after co-transfection with C9orf139 (Fig. 5E).

Extensive studies have shown that the NF-κB pathway is involved in the regulation of immune responses in the body, and it is closely related to cell proliferation and migration. Therefore, we first verified the possible relationship between C9orf139 and the NFκB signaling pathway. After the C9orf139 gene was knocked down, NF-κB and IKK expressions were decreased, and IκB expression was increased. The expression of HDAC11 also decreased correspondingly (Fig. 5F, G). The interaction between NCOR1 and HDAC11 was found by String database analysis (Fig. 5H). WB assay confirmed that decreased expression of C9orf139 gene resulted in decreasing expression of HDAC11 but increasing expression of NCOR1(Fig. 5F, G). Inhibition of miR-661 expression was able to restore some of the effects of C9orf139 knockdown (Fig. 5F, G).

Tumor growth inhibition induced by knockdown of C9orf139 gene in vitro

We constructed a mouse xenograft model through subcutaneous injection to further verify the effect of C9orf139 knockout on tumor growth *in vivo*. TE-1 cells were transfected with NC and shC9orf139-#1 respectively, and then xenografted with mouse xenograft after cell expansion. It was found that, compared with the control group, tumor

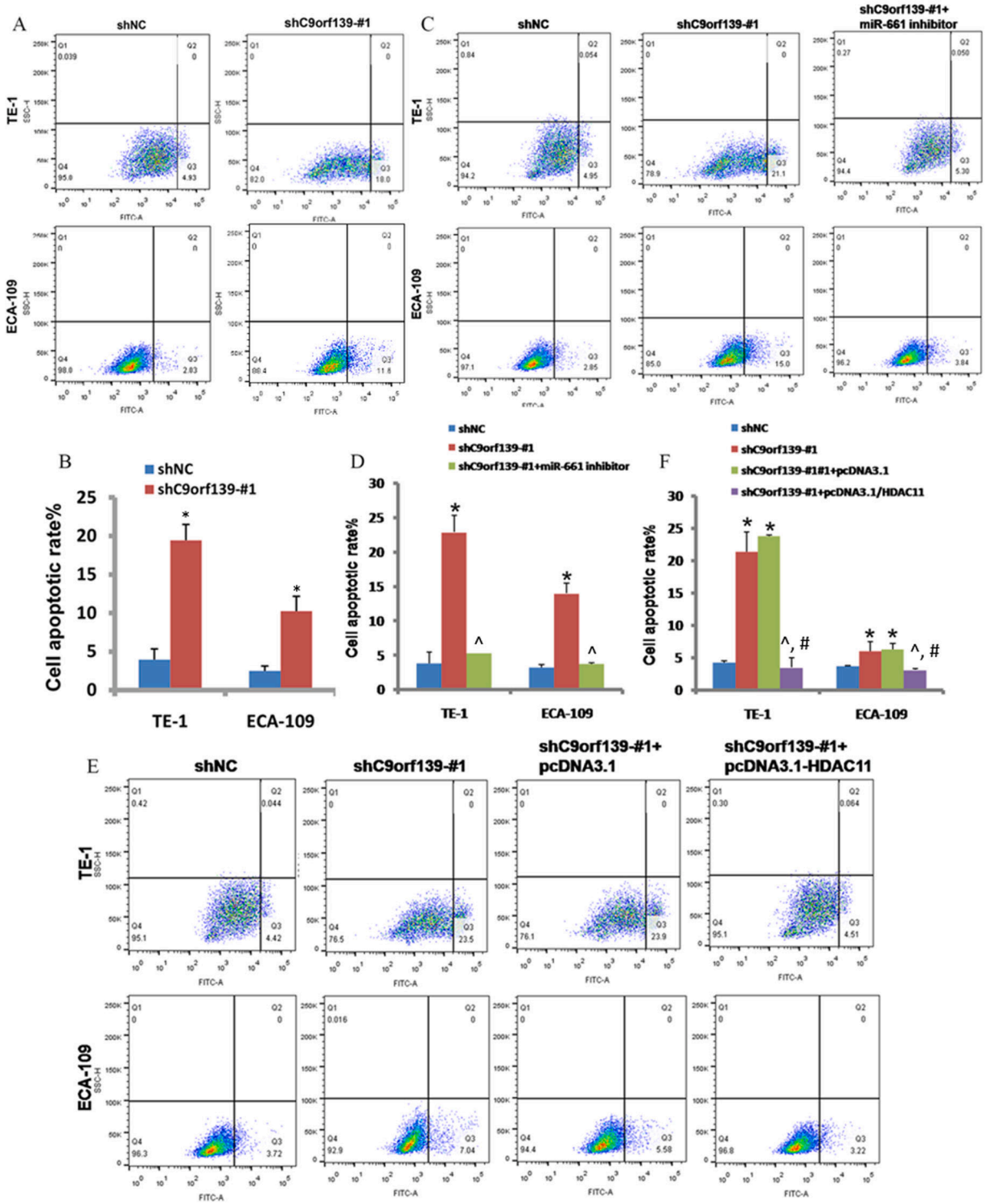

Fig. 4. *C9orf139/miR-661/HDAC11 regulated tumor cell apoptosis.* Apoptosis was detected by Annexin V-FITC assay. (A-B) C9orf139 knockdown resulted in increasing apoptosis: Knockdown of C9orf139 could significantly enhance the apoptosis of esophageal cancer cells. *$p < 0.05$ vs. shNC. (C-D) The apoptosis rate of cancer cells was conspicuously reduced when miR-661 was inhibited. *$p < 0.05$ vs. shNC, ^$p < 0.05$ vs. shC9orfl39#1. (E-F) Knockdown of C9orf139 induced apoptosis of esophageal cancer cells, which was inhibited by overexpression of HDAC11. *$p < 0.05$ vs. shNC, ^$p < p < 0.05$ vs. shC9orfl39#1, #$p < 0.05$ vs. shC9orfl39#1+ pcDNA3.1. The data were presented as mean ± SD.

growth of mice inoculated with shC9orf139-#1-TE-1 cells was slower, tumor volume was significantly reduced, and tumor volume was lighter than that of the control group (Fig. 5I–K).

Discussion

Esophageal cancer (EC) ranks seventh in the incidence of cancers worldwide and sixth in cancer-specific mortality [28]. ESCC accounts for about 90% of all EC histological subtypes [29]. Despite recent

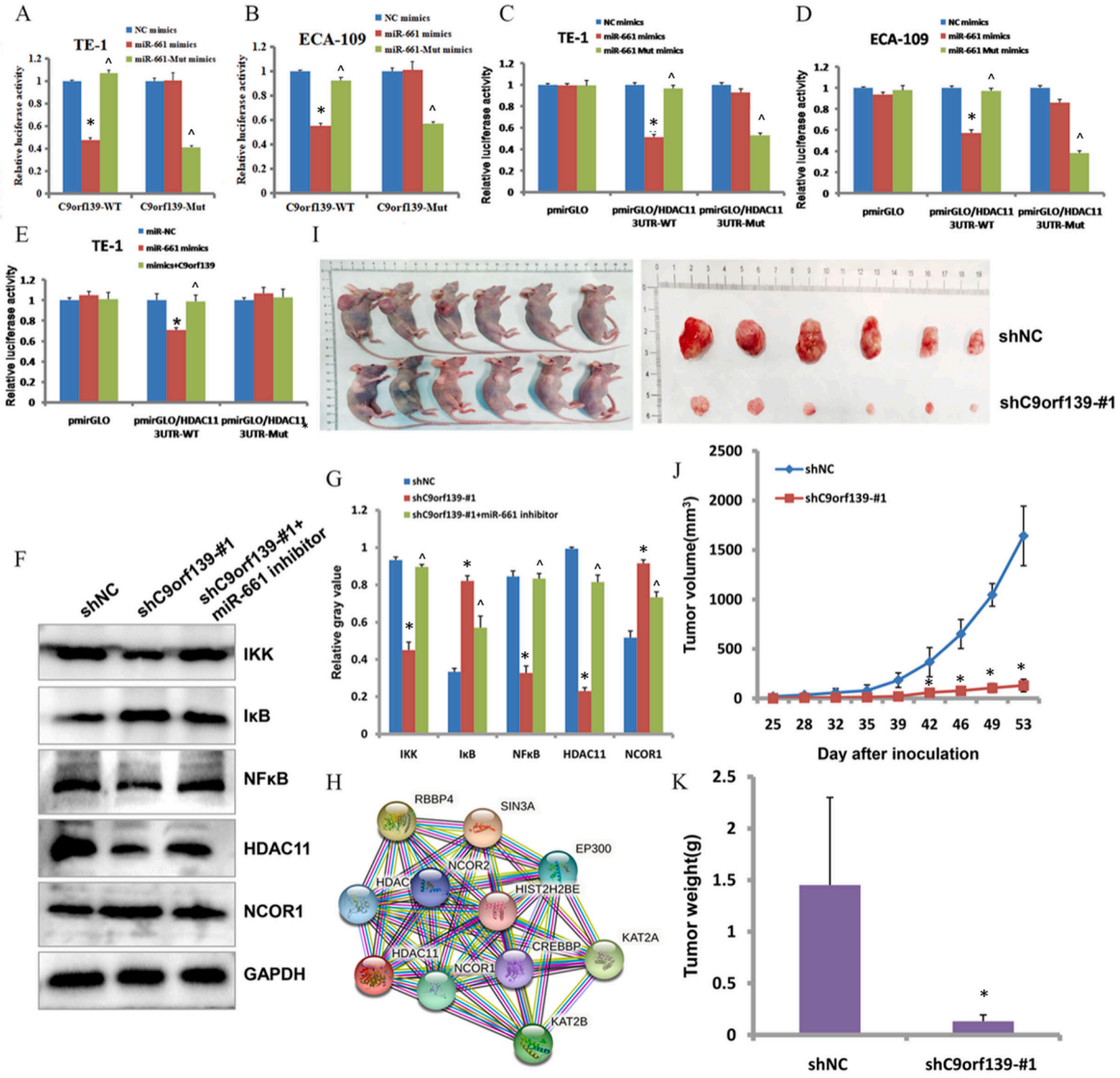

Fig. 5. *Signal transduction mechanism between C9orf139/miR-661/HDAC11 and mouse xenograft model.* (A–E) Double luciferase assay. A-B: miR-661 mimic significantly reduced the expression of luciferase driven by C9orf139, while luciferase expression recovered after site mutation. $*p < 0.05$ vs. NC mimics, $\hat{}p < 0.05$ vs. miR-661 mimics. C-D: miR-661 mimic significantly lessened luciferase expression driven by HDAC11-3-UTR, while luciferase expression recovered after site mutation. $*p < 0.05$ vs. NC mimics, $\hat{}p < 0.05$ vs. miR-661 mimics. E: In TE-1 cells, miR-661 mimic significantly reduced luciferase expression driven by HDAC11-3-UTR, but increased luciferase expression after co-transfection with C9orf139. $*p < 0.05$ vs. NC mimics, $\hat{}p < 0.05$ vs. miR-661 mimics. (F) The regulation of NF-κB signaling pathway by C9orf139/miR-661/HDAC11 was detected by WB. (G) Gray analysis of F. $*p < 0.05$ vs. shNC, $\hat{}p < 0.05$ vs. shC9orfl39#1. (H) String database predicted HDAC11 key interacting proteins. (I) The mice xenograft models and tumors. (J) The volumetric of tumors was measured after removing the tumors from the mice xenograft models. $*p < 0.05$ vs. shNC. (K) Tumor weight of xenograft model mice was measured. $*p < 0.05$ vs. shNC. All data were presented as mean ± SD.

advances in minimally invasive techniques, optimization of chemoradiotherapy protocols, and molecular targeted therapy innovations, ESCC treatment and prognosis of 5-year survival remains low [30,31]. Therefore, it is crucial for the diagnosis and treatment of ESCC to search for molecular targets related to the treatment of ESCC and to further study a series of prognostic indicators that can accurately predict the outcome of surgery, which is the key of the current ESCC research.

In recent years, different kinds of non-coding RNAs have become the focus of research in various fields. In recent years, studies on miRNAs have focused on tumor drug resistance and autophagy [32,33], while LncRNAs are mainly focused on their differential expression and gene regulation functions in different types of cancer [11,34]. More and more studies have found that LncRNAs can act as molecular sponges and interact with miRNAs to regulate gene expression. C9orf139, as an important member of the LncRNA family, has been reported to be associated with the growth of pancreatic cancer cells [17] as well as the prognostic indicators of PDCA patients [18]. Our study confirmed that C9orf139 can regulate downstream HDAC11 expression through interaction with miR-661, and affect the proliferation, invasion, and apoptosis of esophageal cancer tumor cells from both *in vitro* and *in vivo*. The discovery of the C9orf139/miR-661/HDAC11 signaling axis further complicates the role of C9orf139 in the growth and migration of esophageal cancer cells and provides a potential target for the treatment of esophageal cancer.

Previous studies have focused on the regulatory role of immune cells in the NF-κB signaling pathway, and recent studies have found that the NF-κB signaling pathway is closely related to tumor proliferation and migration [35–37]. Dai D et al. demonstrated that PELI1 regulated the

sensitivity of tumor cells to radiotherapy by regulating ir-induced atypical NF-κB expression [38]. In our study, downregulation of C9orf139 resulted in decreasing molecular expression of NF-κB, IKK, and the target gene HDAC11, as well as enhanced expression of IκB, which was restored after inhibition of miR-661. Consistent with previous findings, this study showed that the C9orf139/miR-661/HDAC11 signaling axis was involved in the regulation of NF-κB signaling pathway, and was closely related to the proliferation, invasion and apoptosis of esophageal cancer cells. However, to confirm this hypothesis, further studies should be performed to investigate lncC9orf139 expression in human ESCC tissue and non-cancerous tissue, as well as to explore downstream signaling pathways. MiR-661 overexpression effect on HDAC11C overexpression and the effect of shC9orf139 on other tumor cell lines in regard of apoptosis are also worthy to be determined.

Conclusion

In summary, our study promoted the clarification of the molecular function of C9orf139 and the study of potential therapeutic targets for ESCC, and it provided a new candidate indicator for the prognostic detection of ESCC.

Data availability

All the datas during the current study are included in the article or uploaded as supplementary information.

Ethics approval and consent to participate

The experimental protocols were approved by the Ethics Committee of the Fujian Medical University Union Hospital. This paper has not been published elsewhere in whole or in part. All authors have read and approved the content, and agree to submit it for consideration for publication in your journal. There are no ethical/legal conflicts involved in the article

Funding

This work was supported by Fujian provincial health technology project (2020CX01010103), Fujian Provincial Natural Science Foundation General Project (2021J01745), Fujian Provincial Natural Science Foundation General Project (2020J01997), Young and Middle-aged Teacher Education Research Project of Fujian Education Department (JAT190194) and Sailing Fund General Project of Fujian Medical University (2019QH1023).

CRediT authorship contribution statement

Xiaojie Yang: Conceptualization, Data curation, Formal analysis, Writing – original draft. **Zhimin Shen:** Conceptualization, Data curation, Formal analysis, Writing – original draft. **Mengyue Tian:** Data curation, Formal analysis, Writing – review & editing. **Yukang Lin:** Data curation, Formal analysis. **Liming Li:** Data curation, Formal analysis. **Tianci Chai:** Data curation. **Peipei Zhang:** Methodology. **Mingqiang Kang:** Methodology, Investigation, Data curation, Formal analysis, Visualization, Funding acquisition, Writing – original draft. **Jiangbo Lin:** Methodology, Investigation, Data curation, Formal analysis, Visualization, Funding acquisition, Writing – original draft.

Declaration of Competing Interest

The authors declare that they have no conflicts of interest.

Acknowledgments

Thanks to Alex Ma (ama12@jh.edu) from Johns Hopkins University for proper English language, grammar, punctuation, spelling, and overall style proofreading.

References

[1] S. Kroep, I. Lansdorp-Vogelaar, J.H. Rubenstein, H.J. de Koning, R. Meester, J. M. Inadomi, M. van Ballegooijen, An accurate cancer incidence in Barrett's esophagus: a best estimate using published data and modeling, Gastroenterology 149 (3) (2015) 577–585, https://doi.org/10.1053/j.gastro.2015.04.045, e574quiz e514-575.
[2] J. Xu, D. Kang, M. Xu, S. Zhuo, X. Zhu, J. Chen, Multiphoton microscopic imaging of esophagus during the early phase of tumor progression, Scanning 35 (6) (2013) 387–391, https://doi.org/10.1002/sca.21079.
[3] W. Chen, R. Zheng, P.D. Baade, S. Zhang, H. Zeng, F. Bray, A. Jemal, X.Q. Yu, J. He, Cancer statistics in China, 2015, CA Cancer J. Clin. 66 (2) (2016) 115–132, https://doi.org/10.3322/caac.21338.
[4] H. Liang, J.H. Fan, Y.L. Qiao, Epidemiology, etiology, and prevention of esophageal squamous cell carcinoma in China, Cancer Biol. Med. 14 (1) (2017) 33–41, https://doi.org/10.20892/j.issn.2095-3941.2016.0093.
[5] A. Shafaee, D.Z. Dastyar, J.P. Islamian, M. Hatamian, Inhibition of tumor energy pathways for targeted esophagus cancer therapy, Metabolism 64 (10) (2015) 1193–1198, https://doi.org/10.1016/j.metabol.2015.07.005.
[6] I.E. Khat'kov, R.E. Izrailov, S.A. Domrachev, P.V. Kononets, O.S. Vasnev, M. A. Koshkin, [Thoracolaparoscopic simultaneous operations on esophagus], Khirurgiia (10) (2014) 45–51. Mosk.
[7] C. Allemani, T. Matsuda, V. Di Carlo, R. Harewood, M. Matz, M. Niksic, A. Bonaventure, M. Valkov, C.J. Johnson, J. Esteve, O.J. Ogunbiyi, E.S.G. Azevedo, W.Q. Chen, S. Eser, G. Engholm, C.A. Stiller, A. Monnereau, R.R. Woods, O. Visser, G.H. Lim, J. Aitken, H.K. Weir, M.P. Coleman, C.W. Group, Global surveillance of trends in cancer survival 2000-14 (CONCORD-3): analysis of individual records for 37 513 025 patients diagnosed with one of 18 cancers from 322 population-based registries in 71 countries, Lancet 391 (10125) (2018) 1023–1075, https://doi.org/10.1016/S0140-6736(17)33326-3.
[8] F. Kopp, J.T. Mendell, Functional classification and experimental dissection of long noncoding RNAs, Cell 172 (3) (2018) 393–407, https://doi.org/10.1016/j.cell.2018.01.011.
[9] J.H. Noh, K.M. Kim, W.G. McClusky, K. Abdelmohsen, M. Gorospe, Cytoplasmic functions of long noncoding RNAs, Wiley Interdiscip. Rev. RNA 9 (3) (2018) e1471, https://doi.org/10.1002/wrna.1471.
[10] R. Chen, W.X. Li, Y. Sun, Y. Duan, Q. Li, A.X. Zhang, J.L. Hu, Y.M. Wang, Y.D. Gao, Comprehensive analysis of LncRNA and mRNA expression profiles in lung cancer, Clin. Lab. 63 (2) (2017) 313–320, https://doi.org/10.7754/Clin.Lab.2016.160812.
[11] B. Jiang, B. Yang, Q. Wang, X. Zheng, Y. Guo, W. Lu, LncRNA PVT1 promotes hepatitis B viruspositive liver cancer progression by disturbing histone methylation on the cMyc promoter, Oncol. Rep. 43 (2) (2020) 718–726, https://doi.org/10.3892/or.2019.7444.
[12] L. Jin, H. Fu, J. Quan, X. Pan, T. He, J. Hu, Y. Li, H. Li, Y. Yang, J. Ye, F. Zhang, L. Ni, S. Yang, Y. Lai, Overexpression of long non-coding RNA differentiation antagonizing non-protein coding RNA inhibits the proliferation, migration and invasion and promotes apoptosis of renal cell carcinoma, Mol. Med. Rep. 16 (4) (2017) 4463–4468, https://doi.org/10.3892/mmr.2017.7135.
[13] W.C. Liang, W.M. Fu, C.W. Wong, Y. Wang, W.M. Wang, G.X. Hu, L. Zhang, L. J. Xiao, D.C. Wan, J.F. Zhang, M.M. Waye, The LncRNA H19 promotes epithelial to mesenchymal transition by functioning as miRNA sponges in colorectal cancer, Oncotarget 6 (26) (2015) 22513–22525, https://doi.org/10.18632/oncotarget.4154.
[14] X.S. Wu, F. Wang, H.F. Li, Y.P. Hu, L. Jiang, F. Zhang, M.L. Li, X.A. Wang, Y.P. Jin, Y.J. Zhang, W. Lu, W.G. Wu, Y.J. Shu, H. Weng, Y. Cao, R.F. Bao, H.B. Liang, Z. Wang, Y.C. Zhang, W. Gong, L. Zheng, S.H. Sun, Y.B. Liu, LncRNA-PAGBC acts as a microRNA sponge and promotes gallbladder tumorigenesis, EMBO Rep. 18 (10) (2017) 1837–1853, https://doi.org/10.15252/embr.201744147.
[15] M.D. Paraskevopoulou, A.G. Hatzigeorgiou, Analyzing MiRNA-LncRNA interactions, Methods Mol. Biol. 1402 (2016) 271–286, https://doi.org/10.1007/978-1-4939-3378-5_21.
[16] J. Song, Q. Xu, H. Zhang, X. Yin, C. Zhu, K. Zhao, J. Zhu, Five key LncRNAs considered as prognostic targets for predicting pancreatic ductal adenocarcinoma, J. Cell. Biochem. 119 (6) (2018) 4559–4569, https://doi.org/10.1002/jcb.26598.
[17] J.N. Ge, D. Yan, C.L. Ge, M.J. Wei, LncRNA C9orf139 can regulate the growth of pancreatic cancer by mediating the miR-663a/Sox12 axis, World. J. Gastrointest. Oncol. 12 (11) (2020) 1272–1287, https://doi.org/10.4251/wjgo.v12.i11.1272.
[18] J. Song, Q. Xu, H. Zhang, X. Yin, C. Zhu, K. Zhao, J. Zhu, Five key LncRNAs considered as prognostic targets for predicting pancreatic ductal adenocarcinoma, J. Cell. Biochem. 119 (6) (2018) 4559–4569, https://doi.org/10.1002/jcb.26598.
[19] Y. Zeng, R. Yi, B.R. Cullen, MicroRNAs and small interfering RNAs can inhibit mRNA expression by similar mechanisms, Proc. Natl. Acad. Sci. USA 100 (17) (2003) 9779–9784, https://doi.org/10.1073/pnas.1630797100.
[20] T. Zhu, J. Yuan, Y. Wang, C. Gong, Y. Xie, H. Li, MiR-661 contributed to cell proliferation of human ovarian cancer cells by repressing INPP5J expression, Biomed. Pharmacother. 75 (2015) 123–128, https://doi.org/10.1016/j.biopha.2015.07.023.
[21] Z. Li, Y.H. Liu, H.Y. Diao, J. Ma, Y.L. Yao, MiR-661 inhibits glioma cell proliferation, migration and invasion by targeting hTERT, Biochem. Biophys. Res. Commun. 468 (4) (2015) 870–876, https://doi.org/10.1016/j.bbrc.2015.11.046.
[22] F. Liu, R. Gong, B. He, F. Chen, Z. Hu, TUSC2P suppresses the tumor function of esophageal squamous cell carcinoma by regulating TUSC2 expression and

correlates with disease prognosis, BMC Cancer 18 (2018) 894, https://doi.org/10.1186/s12885-018-4804-9.
[23] J. Huang, L. Wang, S. Dahiya, U.H. Beier, R. Han, A. Samanta, J. Bergman, E. M. Sotomayor, E. Seto, A.P. Kozikowski, W.W. Hancock, Histone/protein deacetylase 11 targeting promotes Foxp^{3+} Treg function, Sci. Rep. 7 (1) (2017) 8626, https://doi.org/10.1038/s41598-017-09211-3.
[24] A. Villagra, F. Cheng, H.W. Wang, I. Suarez, M. Glozak, M. Maurin, D. Nguyen, K. L. Wright, P.W. Atadja, K. Bhalla, J. Pinilla-Ibarz, E. Seto, E.M. Sotomayor, The histone deacetylase HDAC11 regulates the expression of interleukin 10 and immune tolerance, Nat. Immunol. 10 (1) (2009) 92–100, https://doi.org/10.1038/ni.1673.
[25] S. Bhaskara, Histone deacetylase 11 as a key regulator of metabolism and obesity, EBioMedicine 35 (2018) 27–28, https://doi.org/10.1016/j.ebiom.2018.08.008.
[26] H.E. Deubzer, M.C. Schier, I. Oehme, M. Lodrini, B. Haendler, A. Sommer, O. Witt, HDAC11 is a novel drug target in carcinomas, Int. J. Cancer 132 (9) (2013) 2200–2208, https://doi.org/10.1002/ijc.27876.
[27] D. Szklarczyk, A. Franceschini, M. Kuhn, M. Simonovic, A. Roth, P. Minguez, T. Doerks, M. Stark, J. Muller, P. Bork, L.J. Jensen, C. von Mering, The STRING database in 2011: functional interaction networks of proteins, globally integrated and scored, Nucl. Acids Res. 39 (Database issue) (2011) D561–D568, https://doi.org/10.1093/nar/gkq973.
[28] H. Sung, J. Ferlay, R.L. Siegel, M. Laversanne, I. Soerjomataram, A. Jemal, F. Bray, Global cancer statistics 2020: GLOBOCAN estimates of incidence and mortality worldwide for 36 cancers in 185 countries, CA Cancer J. Clin. 71 (3) (2021) 209–249, https://doi.org/10.3322/caac.21660.
[29] GBD 2017 Oesophageal Cancer Collaborators, The global, regional, and national burden of oesophageal cancer and its attributable risk factors in 195 countries and territories, 1990-2017: a systematic analysis for the Global Burden of Disease Study 2017, Lancet Gastroenterol. Hepatol. 5 (6) (2020) 582–597, https://doi.org/10.1016/S2468-1253(20)30007-8.
[30] A. Jemal, R. Siegel, E. Ward, T. Murray, J. Xu, M.J. Thun, Cancer statistics, 2007, CA Cancer J Clin. 57 (1) (2007) 43–66, https://doi.org/10.3322/canjclin.57.1.43.
[31] Q. Wang, L. Peng, Y. Han, T. Li, W. Dai, Y. Wang, L. Wu, Y. Wei, T. Xie, Q. Fang, Q. Li, J. Lang, B. Cao, Preoperative serum sodium level as a prognostic and predictive biomarker for adjuvant therapy in esophageal cancer, Front. Oncol. 10 (2020), 555714, https://doi.org/10.3389/fonc.2020.555714.
[32] Y.H. Lin, MicroRNA networks modulate oxidative stress in cancer, Int. J. Mol. Sci. 20 (18) (2019), https://doi.org/10.3390/ijms20184497.
[33] R. Rupaimoole, F.J. Slack, MicroRNA therapeutics: towards a new era for the management of cancer and other diseases, Nat. Rev. Drug Discov. 16 (3) (2017) 203–222, https://doi.org/10.1038/nrd.2016.246.
[34] S. Jathar, V. Kumar, J. Srivastava, V. Tripathi, Technological developments in LncRNA biology, Adv. Exp. Med. Biol. 1008 (2017) 283–323, https://doi.org/10.1007/978-981-10-5203-3_10.
[35] D.F. Lee, M.C. Hung, Advances in targeting IKK and IKK-related kinases for cancer therapy, Clin. Cancer Res. 14 (18) (2008) 5656–5662, https://doi.org/10.1158/1078-0432.CCR-08-0123.
[36] J. Napetschnig, H. Wu, Molecular basis of NF-kappaB signaling, Annu. Rev. Biophys. 42 (2013) 443–468, https://doi.org/10.1146/annurev-biophys-083012-130338.
[37] S.C. Sun, J.H. Chang, J. Jin, Regulation of nuclear factor-kappaB in autoimmunity, Trends Immunol. 34 (6) (2013) 282–289, https://doi.org/10.1016/j.it.2013.01.004.
[38] D. Dai, H. Zhou, L. Yin, F. Ye, X. Yuan, T. You, X. Zhao, W. Long, D. Wang, X. He, J. Feng, D. Chen, PELI1 promotes radiotherapy sensitivity by inhibiting noncanonical NF-kappaB in esophageal squamous cancer, Mol. Oncol. (2021), https://doi.org/10.1002/1878-0261.13134.